JOURNAL OF BACTERIOLOGY, Mar. 1995, p. 1315–1325 Vol. 177, No. 5
0021-9193/95/$04.00+0

Roles of the Three Transcriptional Attenuators of the *Bacillus subtilis* Pyrimidine Biosynthetic Operon in the Regulation of Its Expression

YANG LU, ROBERT J. TURNER, AND ROBERT L. SWITZER*

Department of Biochemistry, University of Illinois, Urbana, Illinois 61801

Received 17 October 1994/Accepted 31 December 1994

Expression of the *Bacillus subtilis pyr* operon is regulated by exogenous pyrimidines and the protein product of the first gene of the operon, PyrR. It has been proposed that PyrR mediates transcriptional attenuation at three untranslated segments of the operon (R. J. Turner, Y. Lu, and R. L. Switzer, J. Bacteriol., 176:3708–3722, 1994). In this study, transcriptional fusions of the *pyr* promoter followed by the *pyr* attenuation sequences, either individually or in tandem to a *lacZ* reporter gene, were used to examine the physiological functions of all three attenuators through their ability to affect β-galactosidase expression. These fusions were studied as chromosomal integrants in various *B. subtilis* strains to examine the entire range of control by pyrimidines, PyrR dependence, and developmental control of *pyr* gene expression. The nutritional regulation of each attenuator separately was roughly equivalent to that of the other two and was totally dependent upon PyrR, and that of tandem attenuators was cumulative. The regulation of a fusion of the *spac* promoter followed by the *pyrP*:*pyrB* intercistronic region to *lacZ* produced results similar to those obtained with the corresponding fusion containing the *pyr* promoter, demonstrating that attenuator-dependent regulation is independent of the promoter. Extreme pyrimidine starvation gave rise to two- to threefold-higher levels of expression of a *pyr-lacZ* fusion that lacked attenuators, independent of PyrR, than were obtained with cells that were not starved. Increased expression of a similar *spac-lacZ* fusion during pyrimidine starvation was also observed, however, indicating that attenuator-independent regulation is not a specific property of the *pyr* operon. Conversion of the initiator AUG codon in a small open reading frame in the *pyrP*:*pyrB* intercistronic region to UAG reduced expression by about half but did not alter regulation by pyrimidines, which excludes the possibility of a coupled transcription-translation attenuation mechanism. Developmental regulation of *pyr* expression during early stationary phase was found to be dependent upon the attenuators and PyrR, and the participation of Spo0A was excluded.

The genes encoding the enzymes of de novo pyrimidine nucleotide biosynthesis in *Bacillus subtilis* (29, 30, 35, 44) and *Bacillus caldolyticus* (15, 16) are clustered into a 10-cistron operon, which appears to be expressed as a single transcriptional unit. The coding sequences of the *pyr* cluster all overlap by 1 to 32 nucleotides (nt) except at the 5′ end, where three untranslated regions are found (Fig. 1). These regions comprise a 150-nt 5′ leader sequence, a 173-nt intercistronic region between *pyrR* and *pyrP* (*pyrR*:*pyrP*), and a 145-nt intercistronic region between *pyrP* and *pyrB* (*pyrP*:*pyrB*). Examination of the sequences of each of these untranslated regions revealed striking similarities among them (44). Each of them encodes transcripts that are capable of forming stem-loop structures characteristic of transcription terminators. Northern (RNA) hybridization analysis of *pyr* transcripts demonstrated that termination actually does occur in vivo at each of these putative termination sites and that the extent of termination is affected by pyrimidines in the medium (44). The sequences of the three untranslated regions also predicted that *pyr* transcripts are capable of folding to form alternative stable stem-loop structures, which we have termed antiterminators, that would prevent formation of the transcription terminators adjacent to them. Thus, if a mechanism was provided that placed the relative extent of antiterminator stem-loop formation versus terminator formation under the control of intracellular pyrimidine levels, the expression of the *B. subtilis pyr* genes would be regulated by transcriptional attenuation at three sites in the 5′ end of the operon. We have proposed that such a mechanism is provided by the *pyrR*-encoded protein (44). Deletion of *pyrR* leads to constitutive expression of *pyr* genes (44). We have suggested, but not yet proven directly, that the PyrR regulatory protein acts by binding in a pyrimidine nucleotide-dependent fashion to a conserved sequence in the leading stem of each transcript (44). Binding of PyrR is proposed to destabilize the antiterminator, leading to formation of the downstream terminator and transcriptional termination (44). Such a mechanism is analogous to that described for regulation of the *B. subtilis trp* genes by the TRAP protein (3, 17, 27, 34, 39, 40).

The experiments described in this communication were designed to assess the quantitative contribution of each of the three putative attenuation sites in the *pyr* cluster, singly and in combination, to regulation of *pyr* expression by pyrimidines. We also sought to test directly whether each attenuation site was regulated by *pyrR* and to assess the possible significance of a potential internal promoter and a small open reading frame suggested by the sequence of the *pyrP*:*pyrB* intercistronic region. Finally, we have examined the mechanism of the abrupt transcriptional shutoff of *pyr* expression that occurs at the onset of sporulation in rich medium (32) and have shown that this phenomenon also involves *pyrR* and the *pyr* attenuators.

* Corresponding author. Mailing address: Department of Biochemistry, University of Illinois, 600 South Mathews Ave., Urbana, IL 61801. Phone: (217) 333-3940. Fax: (217) 244-5858. Electronic mail address: rswitzer@uiuc.edu.

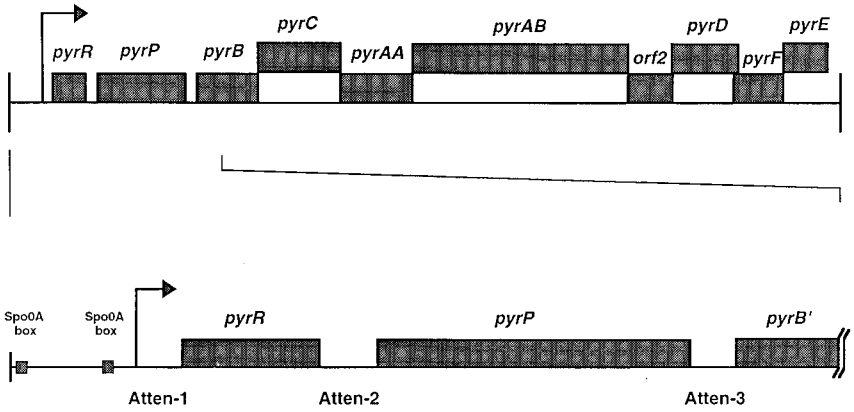

FIG. 1. Structure of the *B. subtilis pyr* operon. The entire gene cluster is shown above the 5′ end presented in expanded form to show the locations of the putative Spo0A boxes 5′ to the *pyr* promoter and of the attenuators (Atten-1, -2, and -3) in the untranslated regions (thin lines). Thick lines denote coding regions. The functions of all the coding sequences except for *orf2* have been identified (35, 44). The complete DNA sequence of the gene cluster is known (30, 35, 44) and has been deposited in the GenBank database under accession number M59757.

MATERIALS AND METHODS

Bacterial strains. The bacterial strains used in this study are listed in Table 1. When pLS47 and other plasmids including only the *pyr* promoter were propagated in *Escherichia coli*, the low-copy-number, *pcnB* host strain KE94 was used because of the instability of these plasmids in the wild-type host strain (35, 44).

Growth media and culture conditions. LB medium (37) was used as a rich liquid medium for *E. coli* and as a solid medium (with 1.5% agar) for both *E. coli* and *B. subtilis*. Supplemented nutrient broth (32) was used as a rich liquid medium for *B. subtilis* and contained 8 g of Difco nutrient broth per liter, 0.1% glucose, and a salt mixture (6). The chemically defined growth medium (6) was based on the medium of Anagnostopoulos and Spizizen (2) and was supplemented with 50% SNB salts (6). The medium contained the following (final concentration): 15 mM $(NH_4)_2SO_4$, 80 mM K_2HPO_4, 44 mM KH_2PO_4, 3.4 mM trisodium citrate, 2.0 mM $MgSO_4$, 6.7 mM KCl, 0.5 mM $CaCl_2$, 5 μM $MnCl_2$, 0.5 μM $FeSO_4$, 0.1% Bacto-Technical Casamino Acids, 1 mg of glucose per ml, and 50 μg of any amino acids needed to meet auxotrophic requirements per ml. To grow *B. subtilis* in the presence of excess pyrimidines, 200 μg of uracil per ml was used. To starve a *B. subtilis pyr* auxotroph for pyrimidines, 40 μg of orotate per ml was used. For a transition from a rich solid medium to a chemically defined liquid medium for *B. subtilis*, a starter culture of Stansly broth (42) was used. *E. coli* pUC- and pBR-based plasmids were selected for with 100 μg of ampicillin per ml. *pyr-lacZ* integrants were selected for with 5 μg of chloramphenicol per ml.

Bacterial transformations. Transformation of *E. coli* was carried out as described by Sambrook et al. (37). *B. subtilis* transformation was carried out by the procedure of Contente and Dubunau (9). Integration of linearized plasmids into the *B. subtilis* chromosome at the *amyE* locus was carried out by the procedures described by Shimotsu and Henner (39) and Lu et al. (31), except that *Pst*I and *Sca*I were used to linearize the plasmids instead of *Pst*I only.

DNA isolation, manipulations, and analysis. Plasmid DNAs from both *E. coli* and *B. subtilis* were isolated as described by Sambrook et al. (37) except that 2 mg of lysozyme per ml was added to solution I when the host was *B. subtilis*. Plasmid DNA was purified by a procedure previously described (43). Chromosomal DNA from *B. subtilis* AG503 (Δ*spo0A*::*cat*) and plasmid pJL62 (*cat*::Spec^r) were kindly supplied by Alan Grossman (Massachusetts Institute of Technology). All enzymes used in the manipulation of DNA were used according to the manufacturer's specifications. DNA was sequenced according to the dideoxynucleotide method of Sanger et al. (38), with the Sequenase version 2.0 kit (United States Biochemical Corp.). PCR was performed with *Taq* DNA polymerase in a Perkin-Elmer Cetus DNA thermal cycler by the procedure recommended by the manufacturer.

Plasmids and construction of *pyr-lacZ* transcriptional fusion integrant strains. Plasmids used in this study are listed in Table 2 or have been described in a previous publication (44).

The plasmids used to produce the *pyr-lacZ* transcriptional fusion integrant *B. subtilis* strains listed in Table 1 were constructed by subcloning various fragments of the *pyr* DNA (see Tables 3 through 7 and Fig. 2) into the vector pDH32 (18), which replicates in *E. coli* but not in *B. subtilis*. pDH32 was designed to permit cloning of a segment of *B. subtilis* DNA in transcriptional fusion to the *E. coli lacZ* gene and to permit integration of the linearized plasmid into the *B. subtilis* chromosome at the *amyE* locus by double crossover. Integrants were selected by their chloramphenicol resistance because the *lacZ* and downstream *cat* genes are flanked by two portions of the *B. subtilis amyE* gene (18, 39). The plasmids were initially constructed in *E. coli* JM83 by selecting for Amp^r with 100 mg of ampicillin per ml. The structures of the plasmids were confirmed by restriction mapping and nucleotide sequencing as needed to establish structures unequivocally. Purified plasmids were linearized by digestion with *Pst*I and *Sca*I and transformed into the appropriate *B. subtilis* host (MO199, HC11, or DB104Δ*pyrR*) by the usual transformation procedures (9); 5 mg of chloramphenicol per ml was used to select for integrants. When an integrant with wild-type chromosomal *pyr* genes was desired, *B. subtilis* MO199 was transformed. Strain MO199, in which the *amyE* gene is disrupted by insertion of a macrolide-lincosamide-streptogramin resistance (MLS^r) gene, became MLS^s after correct integration of a linearized plasmid, which was confirmed on plates containing 1 mg of erythromycin and 20 mg of lincomycin per ml (18). Other *B. subtilis* integrants became AmyE$^-$ and Cm^r, which was confirmed on LB plates supplemented with 1% starch (26) and 5 mg of chloramphenicol per ml. Generally, for each kind of integrant, two to four isolates were selected, grown on the medium indicated, and assayed for β-galactosidase activity. For each isolate, two or three samples were collected at different times during exponential growth and duplicate samples from each time point were assayed. For some integrants, aspartate transcarbamylase activity was also measured to confirm that the integration did not affect the normal regulation of the chromosomal *pyr* gene cluster.

Further details of the methods used to construct pDH32-derived plasmids not previously described (44) are as follows.

pLS45, which includes the *pyr* promoter, the leader region, the *pyrR* gene, the *pyrR*:*pyrP* intercistronic region, and the 5′ half of the *pyrP* gene, was constructed by subcloning a 1.35-kb fragment from pTS183 (44) into pDH32. pTS183 was blunt ended with the Klenow fragment of DNA polymerase after digestion with *Sph*I and was subsequently digested with *Eco*RI. The *Eco*RI-blunt-ended 1.35-kb fragment was then ligated into pDH32 which had been digested with *Bam*HI, blunt ended with the Klenow fragment of DNA polymerase, and then digested with *Eco*RI.

pLS46, which includes all three attenuators, the *pyrR* gene, and part of the *pyrP* gene, was constructed through several steps. Because of the toxicity of overexpressed *pyrP* to both *E. coli* and *B. subtilis* (44), part of the *pyrP* gene was deleted. First, pLS36 was generated by PCR to construct a new *Pst*I site at nt +2126 and a new *Bam*HI site at nt +2819. A 0.71-kb fragment from nt +2117, including a *Pst*I site, to nt +2826, including a *Bam*HI site, was amplified with pLS2 (29) as the template; the 5′ primer was 5′-TCTGCAGACTGCAGGCGAAGGAA GAG-3′ and the 3′ primer was 5′-TGACGGATCCGCATTTGACC-3′ (the *Pst*I and *Bam*HI sites are underlined). The amplified fragment was digested with *Pst*I and *Bam*HI and was ligated into similarly digested pUC18, yielding pLS36. Next, the 0.71-kb *Pst*I-*Sma*I fragment from pLS36 was ligated to pLS35, which has a 1.35-kb *Eco*RI (nt −51)-*Pst*I (nt +1294) fragment from pLS45 and had been treated with *Hin*dIII (Klenow fragment) and *Pst*I, yielding pLS361, from which 828 bp close to the 3′ end of *pyrP* gene was deleted. Finally, the 2.03-kb *Eco*RI-*Bam*HI fragment from pLS361 was ligated into similarly digested pDH32 to generate pLS46.

pLS58, which covers the 3′ end of *pyrP*, the *pyrP*:*pyrB* intercistronic region, and the 5′ end of *pyrB*, was constructed by ligation of the 0.27-kb *Eco*RI-*Bam*HI fragment from pLS382E, which has 250 bp of *pyr* DNA from nt +2132 to +2381 in the *Sma*I site of pUC18, into similarly digested pDH32.

pLS60, which introduces the *pyr* promoter in front of the *pyrP*:*pyrB* intercistronic region, was constructed through several intermediates. First, the 0.71-kb PCR-amplified *Pst*I-*Bam*HI fragment in pLS36 was reoriented in pUC18 by ligating the *Pst*I (mung bean nuclease)-*Bam*HI fragment into the *Bam*HI and *Sma*I sites of pUC18, producing pLS382. A 0.28-kb *Eco*RI-*Sst*I fragment (partially digested with *Sst*I before treatment with mung bean nuclease) was transferred to the *Eco*RI and *Sma*I sites of pUC18, yielding pLS382E, which contains the 3′ end of *pyrP*, the *pyrP*:*pyrB* intercistronic region, and the 5′ end of *pyrB*. The

TABLE 1. Strains used in this study

Strain	Genotype or phenotype	Source (reference)
E. coli		
JM83	ara Δ(*lac-proAB*) *rpsL thi* ϕ80 *lacZ*ΔM15	Laboratory stock (37)
KE94	*hsdS20* ($r_B^-m_B^-$) *recA13 ara-14 proA2 lacY1 galK2 rpsL20 xyl-5 mtl-1 supE44 pcnB80 zad*::Tn*10*	Laboratory stock
B. subtilis		
MO199	*trpC2 pheA amyE*::*erm*	Grandoni et al. (18)
MO207	MO199, *amyE*::pLS47	Turner et al. (44)
MO1991	MO199, *amyE*::pTS290	Turner et al. (44)
MO205	MO199, *amyE*::pLS45	This study
MO206	MO199, *amyE*::pLS46	This study
MO218	MO199, *amyE*::pLS58	This study
MO220	MO199, *amyE*::pLS60	This study
MO222	MO199, *amyE*::pLS62	This study
MO224	MO199, *amyE*::pLS64	This study
MO203	MO199, *amyE*::pLS43	This study
MO204	MO199, *amyE*::pLS44	This study
MO207A	MO199, *amyE*::pLS47 Δ*spo0A*::*cat*	This study
MO203A	MO199, *amyE*::pLS43 Δ*spo0A*::*cat*	This study
HC11	DB104, *pyrB*::Spec^r	Hu and Switzer (25)
DB203	HC11, *amyE*::pLS43	This study
DB207	HC11, *amyE*::pLS47	This study
DB290	HC11, *amyE*::pTS290	This study
DB205	HC11, *amyE*::pLS45	This study
DB206	HC11, *amyE*::pLS46	This study
DB218	HC11, *amyE*::pLS58	This study
DB220	HC11, *amyE*::pLS60	This study
DB222	HC11, *amyE*::pLS62	This study
DB223	HC11, *amyE*::pLS63	This study
DB224	HC11, *amyE*::pLS64	This study
DB225	HC11, *amyE*::pLS65	This study
DB226	HC11, *amyE*::pLS66	This study
DB267	HC11, *amyE*::pLS67	This study
DB104Δ*pyrR*	HC11, *pyrB*$^+$ Spec^s Δ*pyrR*	Turner et al. (44)
DBR207	DB104Δ*pyrR*, *amyE*::pLS47	This study
DBR290	DB104Δ*pyrR*, *amyE*::pTS290	This study
DBR205	DB104Δ*pyrR*, *amyE*::pLS45	This study
DBR220	DB104Δ*pyrR*, *amyE*::pLS60	This study
DBR222	DB104Δ*pyrR*, *amyE*::pLS62	This study
DBR224	DB104Δ*pyrR*, *amyE*::pLS64	This study
DBR225	DB104Δ*pyrR*, *amyE*::pLS65	This study
DB104	*his nprR2 nprE18 ΔaprA3*	Laboratory stock (45)
DBL225	DB104, *amyE*::pLS65	This study
DBL226	DB104, *amyE*::pLS66	This study
DBL267	DB104, *amyE*::pLS67	This study

63-bp *Eco*RI-*Xmn*I fragment containing the *pyr* promoter was then ligated into *Eco*RI-*Kpn*I (mung bean nuclease)-treated pLS382E, yielding pLS601. The final plasmid, pLS60, was then produced by inserting the 0.34-kb *Eco*RI-*Bam*HI fragment from pLS601 into similarly treated pDH32. The structure of the junction areas was confirmed by nucleotide sequencing.

pLS62, which introduces the *pyr* promoter in front of the *pyrR*:*pyrP* intercistronic region, was constructed by several steps also. First, the 0.2-kb *Bam*HI-*Acc*I (Klenow) fragment from pQS800 (35) was ligated into the *Bam*HI and *Sma*I sites of pUC18, producing pLS621. The 63-bp *Eco*RI-*Xmn*I *pyr* promoter was then ligated into *Eco*RI-*Kpn*I (Klenow fragment)-treated pLS621, yielding pLS622. The final plasmid, pLS62, was produced by inserting the 0.26-kb *Eco*RI-*Bam*HI fragment from pLS622 into similarly treated pDH32.

pLS64 is pLS60 with an amber mutation (from AUG to UAG) in the initiation codon for the small open reading frame in the *pyrP*:*pyrB* intercistronic region. The mutation was generated by PCR (44). pLS601 was used as the template. As oligonucleotide primers, a mutagenic 20-mer from nt +2220 to +2201 (5′-CTCTTCTAAACCCTTCCAAG-3′) and the vector primer (5′-AGCGGATAA CAATTTCACACAGGA-3′) were used to introduce the mutation and amplify a 212-bp upstream part of the *pyrP*:*pyrB* intercistronic region. The amplified fragment was then purified by agarose gel electrophoresis. The purified 212-bp fragment was then used as a new primer, along with vector primer 5′-GTTTTC CCAGTCACGAC-3′, to amplify the downstream part of the *pyrP*:*pyrB* intercistronic region. The amplified 0.45-kb fragment was precipitated with ethanol and digested with *Eco*RI and *Bam*HI, and the 0.25-kb fragment was then ligated into pDH32, yielding pLS64. The mutation in the initiation codon was confirmed by DNA sequencing of pLS64.

pLS65, in which the *spac* promoter (47) was fused to the *pyrP*:*pyrB* attenuator and *lacZ*, was constructed through an intermediate plasmid. The 0.29-kb *Eco*RI-*Bam*HI (mung bean nuclease) fragment from pLS661 was ligated into *Eco*RI-*Kpn*I (mung bean nuclease)-treated pLS382E, generating pLS651. The 0.54-kb *Eco*RI-*Bam*HI fragment from pLS651 was then ligated into pDH32, yielding pLS65.

pLS66, in which the *spac* promoter was fused to *lacZ*, was generated by ligating the 0.29-kb *Eco*RI-*Bam*HI fragment from an intermediate plasmid, pLS661, into pDH32. pLS661 was constructed by ligating a 0.29-kb *Eco*RI-*Hin*dIII (Klenow) fragment from pDG148 (22) into *Eco*RI-*Sma*I-treated pUC18.

pLS67, in which the *epr* promoter (7) was fused to the *lacZ* gene, was generated by ligating the 0.70-kb *Eco*RI-*Bam*HI fragment from pWPB183 (7, 44) into pDH32.

Construction of *spo0A* strains. Strain MO203 (Cm^r) was constructed by integrating linearized pLS43, which contains two putative Spo0A boxes and the *pyr* promoter (44), into the chromosome of MO199 at the *amyE* locus. The *cat* gene in MO203 was then disrupted by transformation with linearized pJL62 (19), in which the Spec^r gene is inserted into the *cat* gene, to generate MO303 (Spec^r Cm^s). MO303 was then transformed with the chromosomal DNA from *B. subtilis* AG503 (Δ*spo0A*::*cat*), and Cm^r Spec^r transformants were selected, generating MO203A, which has a Spo0A$^-$ phenotype. The Spo0A$^-$ phenotype was checked by heat treatment of a culture which had been grown into stationary phase at 80°C for 10 min. Percent heat resistance was determined by comparing initial unheated cell counts with cell counts after heating (48). MO207A, which is Spo0A$^-$ and has an insertion of pLS47 at the *amyE* locus, was constructed from MO207 in the same way.

β-Galactosidase assay. β-Galactosidase activity was determined by a modified protocol (19) which is based on Miller's method (33). For cultures grown in the supplemented nutrient broth with glucose medium (21, 32), 1 ml of cell culture was harvested by microcentrifugation and the cell pellet was resuspended in 1 ml of Z buffer (33). The cell density was measured by A_{600}, and the cells were then treated with 10 μl of toluene and were immediately stored at −20°C or were used for β-galactosidase activity assay directly. For cultures grown in buffered minimal medium, the cell density was determined by measuring the A_{600} of the culture without prior centrifugation and 1 ml of the cell culture was treated with 10 μl of toluene and was stored at −20°C or was assayed for β-galactosidase activity directly. Samples (0.1 ml) of the toluenized cells were added to 0.9-ml aliquots of the assay solution (0.1 M sodium phosphate [pH 7.0], 10 mM KCl, 1 mM $MgSO_4$, 50 mM β-mercaptoethanol, and 1 mg of *o*-nitrophenyl-β-D-galactopyranoside per ml) and were incubated at 37°C. The reaction was terminated by adding 0.5 ml of 1 M Na_2CO_3. The A_{420} was read against zero time controls. The specific activity was expressed in Miller units (33). For some isolates, the activity was expressed as A_{420}/ml of culture. The data (see Tables 3 to 7 and Fig. 2) are the averages of three to five determinations taken at different cell densities during growth of the *pyr-lacZ* fusion integrants shown and are shown ± the maximal deviation from the average. Although data from a single growth of a single integrant are shown, usually three independent integrants were isolated and assayed to confirm that the results shown are representative of the type of fusion integrant and growth conditions tested.

Aspartate transcarbamylase activity. Aspartate transcarbamylase was assayed by the procedure described by Bond et al. (6), with 0.4 M Tris-acetate, pH 8.2; a colorimetric determination of carbamylaspartate was used (41).

RESULTS

Regulation of *pyr-lacZ* fusion integrants containing each of the three *pyr* attenuators separately. To investigate the regulation of each of the putative *B. subtilis pyr* attenuators separately, we constructed a series of *pyr-lacZ* transcriptional fusion plasmids in which the *B. subtilis pyr* promoter (nt −51 to +8 relative to the start of transcription, which is at nt +1) was fused to segments of *pyr* DNA encoding the first, second, or third attenuator and the resultant constructs were then fused to the ribosome binding site and complete coding sequence of the *E. coli lacZ* gene. These plasmids were integrated into the *B. subtilis* chromosome at the *amyE* locus, as described in Materials and Methods. The site of integration is quite far away on the *B. subtilis* chromosome from the *pyr* gene cluster (1), so the chromosomal *pyr* genes were not perturbed. The regulation of *pyr-lacZ* expression was first examined with cells

TABLE 2. Plasmids used in this study

Plasmid	Characteristic(s)	Reference
pUC18	Ap^r	Yanisch-Perron et al. (46)
pLS35	1.35 kb of *Eco*RI-*Pst*I fragment from pLS45 in pUC18	This study
pLS36	0.70-kb PCR-amplified *Pst*I-*Bam*HI fragment, covering 3′ part of *pyrP*, *pyrP*:*pyrB* intercistronic region, and 5′ part of *pyrB*, in pUC18	This study
pLS361	0.70-kb *Pst*I-*Sma*I fragment from pLS36 in *Pst*I-*Hin*dIII (Klenow) sites of pLS35. 0.83 kb of the 3′ portion of *pyrP* was removed in this construction	This study
pLS382	0.70-kb *Pst*I (mung bean nuclease)-*Bam*HI fragment from pLS36 in *Sma*I-*Bam*HI sites of pUC18	This study
pLS382E	0.27-kb *Eco*RI-*Sst*I (mung bean nuclease) fragment from pLS382 in *Eco*RI-*Sma*I sites of pUC18. This plasmid contains 3′ end of *pyrP*, *pyrP*:*pyrB* intercistronic region, and 5′ end of *pyrB*	This study
pLS601	0.063-kb *Eco*RI-*Xmn*I *pyr* promoter in *Eco*RI-*Kpn*I (mung bean nuclease)-treated pLS382E. In this plasmid, the *pyr* promoter was introduced into the *pyrP*:*pyrB* intercistronic region	This study
pLS621	0.2-kb *Bam*HI-*Acc*I (Klenow) fragment from pQS800 (35) in *Bam*HI-*Sma*I sites of pUC18	This study
pLS622	0.063-kb *Eco*RI-*Xmn*I *pyr* promoter in *Eco*RI-*Kpn*I (mung bean nuclease) sites of pLS621. In this plasmid, the *pyr* promoter was introduced into the *pyrR*:*pyrP* intercistronic region	This study
pLS641	pLS601 with an amber mutation (from AUG to UAG) in the start codon for the short open reading frame which encodes a 19-aa peptide in the *pyrP*:*pyrB* intercistronic region[a]	This study
pLS651	0.29-kb *Eco*RI-*Hin*dIII (Klenow) fragment including *spac* promoter from pDG148 in *Eco*RI-*Kpn*I (mung bean nuclease)-treated pLS382E	This study
pLS661	0.29-kb *Eco*RI-*Hin*dIII (Klenow) fragment including *spac* promoter from pDG148 in *Eco*RI-*Sma*I-treated pUC18	This study
pDH32	Ap^r Cm^r *amyE* front, *amyE* back, *lacZ*	Grandoni et al. (18)
pLS43	0.61-kb *Eco*RI-*Bss*HII (Klenow) fragment of pQS18CP (35), containing the *pyr* promoter and upstream region, in the *Eco*RI-*Bam*HI (Klenow) sites of pDH32	Turner et al. (44)
pLS44	0.2-kb *Eco*RI-*Bam*HI fragment from pLS34 (44) in pDH32	Turner et al. (44)
pLS47	0.13-kb *Eco*RI-*Bam*HI fragment from pLS372 (44) in pDH32	Turner et al. (44)
pTS290	0.28-kb *Eco*RI-*Bam*HI fragment from pUC19/290 (44) in pDH32	Turner et al. (44)
pLS45	1.35-kb *Eco*RI-*Sph*I (Klenow) fragment from pTS183 (44) in pDH32, which was treated with *Eco*RI and *Bam*HI (Klenow fragment)	This study
pLS46	2.03 kb of *Eco*RI-*Bam*HI fragment from pLS361 in pDH32	This study
pLS58	0.28-kb *Eco*RI-*Bam*HI fragment from pLS382E in pDH32	This study
pLS60	0.33-kb *Eco*RI-*Bam*HI fragment from pLS601 in pDH32	This study
pLS62	0.26-kb *Eco*RI-*Bam*HI fragment from pLS622 in pDH32	This study
pLS64	0.34-kb *Eco*RI-*Bam*HI fragment from pLS641 in pDH32	This study
pLS65	0.56-kb *Eco*RI-*Bam*HI fragment from pLS651 which includes *spac* promoter-*pyr* attenuator-*lacZ* fusion in pDH32	This study
pLS66	0.29-kb *Eco*RI-*Bam*HI fragment from pLS661 which includes *spac* promoter in pDH32	This study
pLS67	0.70-kb *Eco*RI-*Bam*HI fragment including *epr* promoter from pWPB183 in pDH32	This study

[a] aa, amino acid.

with normal *pyr* genes that had been grown on defined medium with excess uracil (0.2 mg/ml) or with no added pyrimidines (Table 3, part A). Under these conditions the repression of aspartate transcarbamylase (encoded by *pyrB*, which is downstream from all three attenuators) is about 6- to 10-fold (data not shown). A *pyr-lacZ* fusion in which the *pyr* promoter with no attenuator (nt −51 to +72) was joined to *lacZ* showed constitutive β-galactosidase expression (Table 3, MO207), whereas a fusion linking the promoter and the 5′ leader attenuator (nt −51 to +230) to *lacZ* was repressed threefold by uracil (Table 3, MO1991). When fusions containing the *pyr* promoter (nt −51 to +8) linked to the second attenuator (nt +656 to +848) or to the third attenuator (nt +2132 to +2381) and then to *lacZ* were examined, the extent of repression was three- to fivefold (Table 3, MO222 and MO220). Each of the attenuators was regulated by excess pyrimidines to about the same extent as the others, but no single attenuator was repressed as much as aspartate transcarbamylase activity or as *pyr-lacZ* fusions containing three *pyr* attenuators in tandem (as detailed below). With all three fusion integrant strains, the level of β-galactosidase was lower in cells grown without pyrimidines than in cells in which the *pyrR* gene had been deleted (Table 3, part B). This result suggests that endogenous pyrimidine levels are sufficiently high in wild-type cells grown on minimal medium to exert significant repression.

To examine regulation of the attenuators under conditions of pyrimidine limitation, the *pyr-lacZ* fusions were integrated into the *amyE* locus of *B. subtilis* HC11, a Δ*pyrB*::$Spec^r$ pyrimidine auxotroph. Levels of β-galactosidase were determined in cells grown with excess uracil and with 40 μg of orotate per ml, a condition that leads to slow growth and extreme pyrimidine starvation because orotate enters the cells very poorly. Under these conditions, in other Pyr^- mutants derepression of aspartate transcarbamylase is about 200-fold. The repressed levels of *pyr-lacZ* expression in these strains were, as expected, similar to those seen with the same fusion integrants in Pyr^+ cells (Table 3, parts A and C). However, pyrimidine starvation resulted in strong derepression, 40- to 60-fold, of each integrant and much higher levels of β-galactosidase than those seen when Pyr^+ cells were grown without pyrimidines. Thus, the full capacity of each of the three individual attenuators to be regulated by intracellular pyrimidines is similar to that of the other two and can be observed only as a result of pyrimidine starvation. Unexpectedly, the level of expression of a fusion containing no attenuators was 2.5-fold higher during pyrimidine starvation than when the cells were grown with excess uracil (Table 3, DB207). This attenuator-independent regulation was consistently observed; we discuss possible mechanisms below.

Deletion of the *pyrR* gene was previously shown to lead to

TABLE 3. Expression of *pyr-lacZ* fusion integrants containing the three *pyr* attenuators separately[a]

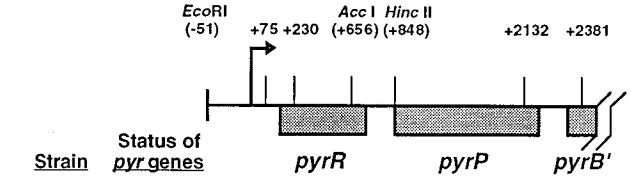

Strain	Status of *pyr* genes	β-Galactosidase Activity[b] (Miller Units) -Uracil	+Uracil	-U/+U
A.				
MO207	WT	228±55	228±63	1
MO1991	WT	89±7	28±8	3
MO222	WT	143±48[c]	52±22[c]	3
MO220	WT	159±32	30±6	5
B.				
DBR207	Δ*pyrR*	313±55	292±18	1
DBR290	Δ*pyrR*	314±61	294±55	1
DBR222	Δ*pyrR*	316±41	324±33	1
DBR220	Δ*pyrR*	586±80	538±38	1
C.		+Orotate[d]	+Uracil	+O/+U
DB207	Δ*pyrB*	720±125	285±31	2.5
DB290	Δ*pyrB*	825±64	17±3	48
DB222	Δ*pyrB*	1,450±54	54±22[c]	38
DB220	Δ*pyrB*	2,065±57	36±18	57

[a] To indicate the portions of *B. subtilis pyr* DNA that were fused to *lacZ*, a schematic map of the 5′ end of the *pyr* operon is drawn at the top of the table. Segments shown below by heavy lines were fused to the *lacZ* gene. When the *pyr* promoter was not normally adjacent to the *pyr* segment used (in the case of the second and third attenuators), the *pyr* promoter (nt −51 to +8) was fused 5′ to the segment shown and is shown by light lines. WT, wild type.

[b] Cultures were grown in buffered minimal medium in the absence of pyrimidines or in the presence of 0.2 mg of uracil (U) per ml or 0.04 mg of orotate (O) per ml as indicated. Values indicate averages ± maximal deviations.

[c] Miller units declined when the cell density increased.

[d] Growth of the Δ*pyrB* strain on orotate as the sole pyrimidine source results in slow growth and extreme pyrimidine starvation.

high levels of constitutive expression of aspartate transcarbamylase (44). To test whether each of the three *pyr* attenuators is regulated by PyrR, the *pyr-lacZ* fusions described above were integrated into the *amyE* locus of a Δ*pyrR* strain. The fusion integrant strains were grown with and without excess uracil, and β-galactosidase activities were measured (Table 3, part B). With all integrants, constitutive expression of β-galactosidase was observed. Thus, each of the attenuators absolutely requires PyrR for regulation by pyrimidines. The level of expression in Δ*pyrR* strains was always less than half of that seen when the same fusions were starved for pyrimidines in Δ*pyrB pyrR*$^+$ cells, however (Table 3, parts B and C). This observation again indicates an attenuator-independent mechanism of regulation.

Regulation of *pyr-lacZ* fusion integrants containing the *pyr* attenuators in tandem. The preceding experiments indicated that each of the three *pyr* attenuators is regulated in a *pyrR*-dependent fashion to approximately the same extent by intracellular pyrimidines. To test how the attenuators function when they are linked in tandem separated by the *pyrR* and *pyrP* genes as they occur normally in the *pyr* operon, two additional *pyr-lacZ* fusions containing two and three attenuators were constructed and regulation of their expression was compared to that of fusions with no attenuator or one attenuator, as already described. The *pyr-lacZ* fusion containing two attenuators also included the *pyrR* gene and the N-terminal portion of the *pyrP* gene (Table 4, MO205 and DB205, nt −51 to +1294). The *pyr-lacZ* fusion containing three attenuators included all of the *pyr* DNA from the promoter to the N-terminal segment of *pyrB* (Table 4, MO206 and DB206, nt −51 to +2381) transcriptionally fused to *lacZ*, except that a segment of *pyrP* (nt +1294 to +2132) was deleted. It was necessary to delete part of *pyrP* because the toxicity of the plasmid-encoded *pyrP* gene in *E. coli* (35, 44) prevented construction of fusions encoding the intact gene. These fusions were integrated into the *amyE* locus of *B. subtilis* MO199 (*pyr*$^+$) and HC11 (Δ*pyrB*), and regulation of β-galactosidase expression by pyrimidines was examined.

The results indicate that regulation of the *pyr* genes by tandem attenuators is cumulative (Table 4). That is, no repression occurred without an attenuator, significant repression was seen with a single attenuator, and further repression was observed when the first and second attenuators were linked in tandem. Our experiments did not clearly demonstrate additional re-

TABLE 4. Expression of *pyr-lacZ* fusion integrants containing the *pyr* attenuators in tandem

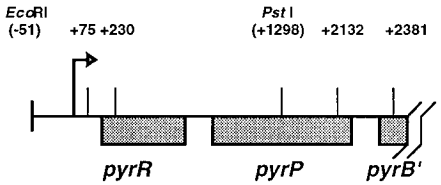

Strain	Status of *pyr* genes	Number of Attenuators	β-Galactosidase Activity[a] (Miller Units) -Uracil	+Uracil	-U/+U
A.					
MO207	WT	0	319±46	304±40	1
MO1991	WT	1	89±7	28±8	3
MO205	WT	2	56±4	10±6	5
MO206	WT	3	106±18	16±11	6
B.			+Orotate[b]	+Uracil	+O/+U
DB207	Δ*pyrB*	0	744±156	305±26	2.4
DB290	Δ*pyrB*	1	794±160	18±6	44
DB205	Δ*pyrB*	2	681±51	2±1	340
DB206	Δ*pyrB*	3	1,046±96	2±1	500

[a] Cultures were grown in the absence or presence of 0.2 mg of uracil per ml for MO (wild-type [WT]) strains, or in the presence of 0.04 mg of orotate (O) per ml or 0.2 mg of uracil (U) per ml for DB strains. Values indicate averages ± maximal deviations.
[b] Growth of the Δ*pyrB* strain on orotate results in slow growth and pyrimidine starvation.

pression in the *pyr-lacZ* fusion containing three attenuators, but this might have been difficult to detect given the low levels of β-galactosidase produced. The results suggest that virtually all of the *pyr* transcripts are terminated by the time the third attenuator is transcribed when the cells are grown on excess uracil. On the other hand, when the fusion integrant strains were starved for pyrimidines (Table 4, part B), very high levels of β-galactosidase were produced. This result indicates that very little transcriptional termination occurs at any of the terminators under these conditions.

Possible additional roles of the *pyrP:pyrB* intercistronic region in the regulation of the *pyr* operon. Quinn et al. (35) pointed out two features of the *pyrP:pyrB* intercistronic region that suggested possible additional elements in the regulation of *pyr* operon expression. The first of these was a putative promoter sequence centered at the very end of *pyrP*. Transcripts initiated at this promoter could not be detected by either primer extension or S1 nuclease protection experiments, but multicopy promoter-indicator plasmids bearing this region had weak promoter activity (35). *pyr-lacZ* fusion integrants in which the intercistronic region only (nt +2132 to +2381) with no *pyr* promoter was transcriptionally fused to *lacZ* were constructed. These strains produced no more detectable β-galactosidase activity than integrants of the vector pDH32 alone, even under conditions of pyrimidine starvation (Table 5, MO218 and DB218). We conclude that there is no functional secondary *pyr* promoter in the *pyrP:pyrB* intercistronic region.

The second feature in this intercistronic region noted by Lerner and Switzer (30) and by Quinn et al. (35) is a potential small (20-codon) open reading frame following a possible ribosome binding site located between *pyrP* and *pyrB*. This open reading frame is positioned relative to a transcriptional terminator quite similarly to the open reading frame for the leader peptide of the *E. coli pyrBI* operon, which is known to be regulated by a coupled transcription-translation attenuation mechanism (28, 36). We sought to evaluate the possible role of translation of the short open reading frame in the *B. subtilis pyrP:pyrB* intercistronic region in regulation by constructing a mutant form of the corresponding *pyr-lacZ* fusion in which the AUG translation initiation codon in strains MO220, DBR220, and DB220 was converted to a UAG termination codon (Table 5, strains MO224, DBR224, and DB224). The ability of these AUG-to-UAG mutant *pyr-lacZ* fusion integrants to be regulated by pyrimidines was essentially the same as that of the parent fusion integrants, whether growth with excess uracil was compared with growth on minimal medium (Table 5, MO220 versus MO224) or with extreme pyrimidine starvation (Table 5, DB220 versus DB224). As expected, the requirement for an intact *pyrR* gene was retained in the AUG-to-UAG mutant (Table 5, DBR220 versus DBR224). Overall expression of β-galactosidase was reduced by about 2.5-fold by the introduction of the termination codon, except in pyrimidine-starved cells, where it was reduced by only 1.5-fold. In this last case, the effect of the mutation may be partially masked by the phenomenon of attenuator-independent derepression (as discussed above). The results indicate that translation of the 20-codon reading frame in the *pyrP:pyrB* intercistronic region is not necessary for transcriptional readthrough and plays no role in regulation of attenuation by pyrimidines. Our results are in contrast to those of Roland et al. (36), who introduced a series of translation termination mutations into the coding sequence for the *E. coli pyrBI* leader polypeptide and observed strong reductions in readthrough (5- to 20-fold) when ochre codons replaced codons in the N-terminal region of the leader peptide.

The reduction in *pyr-lacZ* expression in the AUG-to-UAG mutant fusion integrants may also offer an explanation for the greater expression of the *pyr-lacZ* fusions that include the

TABLE 5. Potential roles of the *pyrP:pyrB* intercistronic region in the expression of *pyr-lacZ* fusion integrants[a]

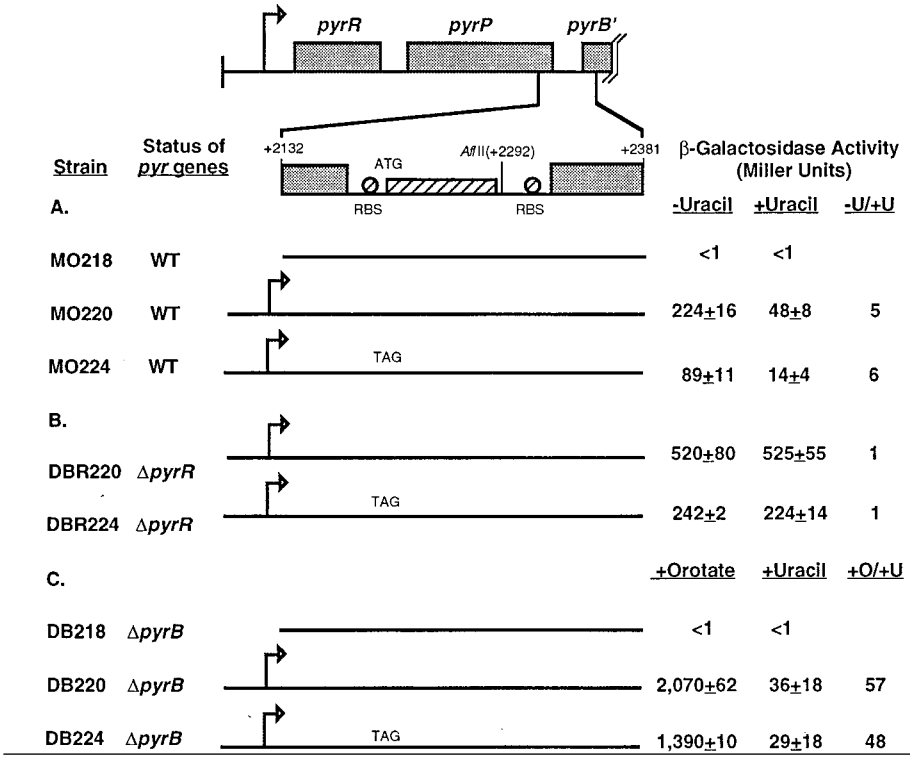

Strain	Status of *pyr* genes	β-Galactosidase Activity (Miller Units)		
A.		-Uracil	+Uracil	-U/+U
MO218	WT	<1	<1	
MO220	WT	224±16	48±8	5
MO224	WT	89±11	14±4	6
B.				
DBR220	Δ*pyrR*	520±80	525±55	1
DBR224	Δ*pyrR*	242±2	224±14	1
C.		+Orotate	+Uracil	+O/+U
DB218	Δ*pyrB*	<1	<1	
DB220	Δ*pyrB*	2,070±62	36±18	57
DB224	Δ*pyrB*	1,390±10	29±18	48

[a] The conditions of the experiment and the symbols used in the table are as described in Table 3, footnotes *a* and *b*. RBS, ribosome binding site.

pyrP:pyrB intercistronic region, compared with the fusions containing the other untranslated regions of the *pyr* operon (Table 3). The replacement of the translational start codon with a termination codon in every case reduced expression of the fusion integrants to values similar to those seen with the other fusion integrants. This observation suggests that ribosomes bind to the *pyrP:pyrB* intercistronic reading frame and translate it. Translation has little effect on regulation of the attenuator by *pyrR*, but it could increase the expression of downstream genes, either by increasing the efficiency of ribosome loading at this point in the mRNA or by protection of the mRNA against degradation in vivo. The possibility also exists that reduced expression of the AUG-to-UAG mutant fusion integrants results directly from altered mRNA structure or stability rather than from failure to translate the *pyrP:pyrB* intercistronic open reading frame.

Does the *pyr* promoter or its 5′ flanking region play any role in regulation of the *pyr* operon by pyrimidines? The model previously proposed for control of the *pyr* operon by attenuation involves only the action of the PyrR protein (and a pyrimidine nucleotide) at the three attenuation sites downstream from the *pyr* promoter (44). Most of the observations in the preceding sections support this model. However, the observation of attenuator-independent regulation in strains subjected to severe pyrimidine limitation led us to investigate whether attenuation control might be supplemented by the action of a repressor protein or another mechanism that regulates the frequency of transcriptional initiation via interactions at the promoter or the 5′ region flanking it. *pyr-lacZ* transcriptional fusion integrants including the 539 bp of *B. subtilis* DNA lying 5′ to the start of *pyr* transcription (MO203) or 160 bp of 5′ flanking DNA (MO204) were compared to a fusion integrant containing the *pyr* promoter only (MO207, which carries nt −51 to +72 of *pyr* DNA). Although the fusion integrants containing additional flanking DNA consistently expressed 20 to 35% more β-galactosidase than strain MO207, none of the fusions were repressible by exogenous pyrimidines (Table 6, part A). The fusion containing the longest 5′ flanking sequence and the fusion containing the *pyr* promoter only were also integrated into strain HC11 (Δ*pyrB*), and β-galactosidase expression during pyrimidine starvation of the resulting integrants, DB203 and DB207, was measured (Table 6, part B). The extent of attenuator-independent derepression during pyrimidine starvation was the same in both strains, 2- to 2.5-fold. These results indicate that the sequences from nt −539 to −51 flanking the promoter play no role in regulation of the operon by pyrimidines.

We next examined the consequences of replacing the normal *pyr* promoter with other *B. subtilis* promoters on regulation of *lacZ* fusion integrants by pyrimidines. As described above, a *pyr-lacZ* fusion lacking an attenuator was not repressible by uracil, but yielded 2.5-fold-increased expression during pyrimidine starvation. Fusions of the *B. subtilis epr* (7) and *spac* (47) promoters to *lacZ* were integrated into the chromosome of the same *B. subtilis* strains used in the preceding studies, and β-galactosidase expression was measured. None of these fusion integrants were repressed by uracil, as expected (Table 7). However, during extreme pyrimidine limitation caused by growth of a Δ*pyrB* strain on orotate, the fusions showed significant effects which differed from promoter to promoter. The *spac-lacZ* fusion yielded an even greater increase in expression during pyrimidine starvation than the *pyr-lacZ* fusion (Table

TABLE 6. Effects of 5′ flanking sequences on expression of *pyr* promoter-*lacZ* fusion integrants[a]

Strain	Status of *pyr* genes	Number of Spo0A Boxes	β-Galactosidase Activity (Miller Units)		
			-Uracil	+Uracil	-U/+U
A.					
MO203	WT	2	273±7	264±6	1.0
MO204	WT	1	311±9	285±17	1.1
MO207	WT	0	240±14	299±60	0.8
B.			+Orotate	+Uracil	+O/+U
DB203	Δ*pyrB*	2	784±60	380±35	2.1
DB207	Δ*pyrB*	0	718±227	285±31	2.5

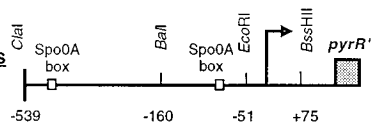

[a] The conditions of the experiment and the symbols used in the table are as described in Table 3 footnotes *a* and *b*.

7). On the other hand, expression of the *epr-lacZ* fusion was sharply decreased under the same conditions. The mechanisms that account for these effects are unknown, but the results indicate that what we have termed attenuator-independent regulation of *pyr-lacZ* fusions is not a specific regulatory mechanism involving the *pyr* promoter but rather an effect of extreme pyrimidine limitation or of slow growth on transcription that affects different promoters quite differently.

As a further test of the proposal that regulation of the *pyr* operon involves only the attenuators and PyrR protein, we constructed a fusion in which the *spac* promoter rather than the *pyr* promoter was joined to the *pyrP:pyrB* attenuator and then to *lacZ* and regulation of β-galactosidase expression was studied (Fig. 2). The results should be compared with those for equivalent fusion integrants that contained the *pyr* promoter (Table 3, MO220, DBR220, and DB220). For all integrants, the amount of β-galactosidase produced was significantly less with the *spac* promoter than with the *pyr* promoter but the extent of regulation by exogenous pyrimidines, the requirement for an intact *pyrR* gene, and extreme derepression during pyrimidine starvation were quite similar with both promoters. The greater derepression seen during pyrimidine starvation with the *spac* promoter than with the *pyr* promoter presumably reflects the fourfold greater sensitivity of the *spac* promoter to the effects of extreme pyrimidine limitation noted in the previous paragraph and in Table 7. These results document conclusively that the regulation of expression by the *pyrR*-encoded protein and *pyr* attenuators is completely independent of the *pyr* promoter or any DNA sequence flanking it.

Regulation of *pyr* operon expression during early sporulation in rich medium. The synthesis of aspartate transcarbamylase has been shown to cease abruptly during the first 2 h of the stationary phase of growth of *B. subtilis* cells on rich medium, conditions that lead to efficient sporulation (32). This cessation of synthesis of aspartate transcarbamylase apparently results from a transcriptional control mechanism, because *pyrB*-encoding transcripts could no longer be detected by hybridization in extracts of cells harvested 1 h after the end of exponential growth (35). Quinn et al. (35) noted the presence of a consensus binding site for the Spo0A transcription regulatory protein located at about nt −100 relative to the start of *pyr* transcription. They suggested that *pyr* transcription during early sporulation might be regulated by *spo0A* and the phosphorelay system which has been shown to regulate expression of a number of other genes during the transition from exponential growth to stationary phase (8). Subsequently, we noted the presence of another consensus Spo0A binding site, TGGCGAA, centered at nt −504. To test whether these Spo0A boxes play a role in the developmental shutoff of *pyr* transcription, the 5′ flanking DNA including both of the putative Spo0A binding sites and the *pyr* promoter (nt −539 to +72) was fused to *lacZ* and integrated into *B. subtilis* MO199 at the *amyE* locus, yielding MO203 (Table 6). The production of β-galactosidase during exponential and stationary phases of growth on rich medium by

TABLE 7. Expression of promoter-*lacZ* fusion integrants in *B. subtilis*

Promoter	Strain	Status of *pyr* genes	β-Galactosidase activity[a] (Miller units)			Strain	Status of *pyr* genes	β-Galactosidase activity (Miller units)		
			−Uracil	+Uracil	−U/+U			+Orotate	+Uracil	+O/+U
pyr	MO207	WT[b]	319 ± 46	304 ± 40	1.0	DB207	Δ*pyrB*	720 ± 125	285 ± 3	2.5
epr	DBL267	WT[c]	37 ± 8	37 ± 8	1.0	DB267	Δ*pyrB*	6 ± 1	56 ± 9	0.1
spac	DBL226	WT[c]	69 ± 4	58 ± 1	1.2	DB226	Δ*pyrB*	744 ± 53	78 ± 1	9.5

[a] Values indicate averages ± maximal deviations. U, uracil; O, orotate.
[b] Host strain is MO199. WT, wild type.
[c] Host strain is DB104.

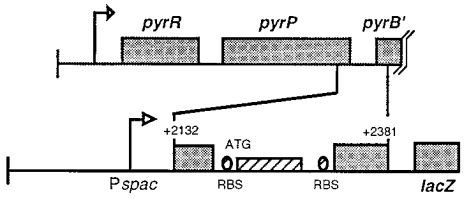

Strain	Status of *pyr* genes	β-Galactosidase Activity (Miller Units) -Uracil	+Uracil	-U/+U
DBL225	WT	27±8	4±1	6.3
DBR225	Δ*pyrR*	107±17	108±18	1.0
		+Orotate	+Uracil	+O/+U
DB225	Δ*pyrB*	954±224	3±2	300

FIG. 2. β-Galactosidase expression of P*spac-pyrP:pyrB* attenuator-*lacZ* fusion integrants. The function of the *pyr* attenuators is independent of the promoter. RBS, ribosome binding site; WT, wild type; U, uracil; O, orotate. The numbers above the diagram indicate nucleotide positions. The activities shown are averages ± maximal deviations.

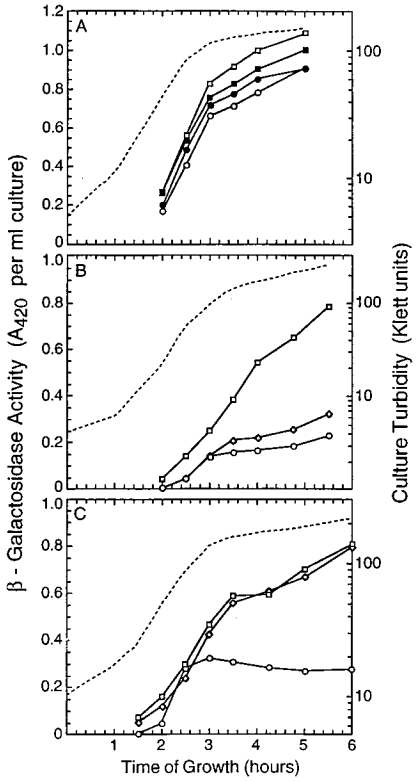

FIG. 3. Use of *pyr-lacZ* fusion integrants to assess the role of Spo0A binding sites and the *spo0A* gene (A), the first two *pyr* attenuators (B), and the *pyrR* gene (C) in developmental regulation of *pyr* expression during early stationary phase after growth on rich medium at 37°C. The *B. subtilis* strains indicated were grown on rich medium (32), the turbidity of the culture was determined with a Klett colorimeter (no. 66 filter) (dashed lines), and the accumulation of β-galactosidase activity in the cells (solid lines) was measured during exponential growth and early stationary phase due to glucose exhaustion. (A) β-Galactosidase activities accumulated by strain MO203, a *pyr-lacZ* fusion including two Spo0A boxes 5′ to the *pyr* promoter (□), and strain MO207, a *pyr-lacZ* fusion with no Spo0A box (○), are compared with activities accumulated by isogenic Δ*spo0A*::*cat* disruption mutants MO203A (■) and MO207A (●), respectively. (B) β-Galactosidase activities accumulated by strain MO207, a *pyr-lacZ* fusion with no downstream attenuator (□); strain MO1991, a *pyr-lacZ* fusion including the *pyr* promoter and the 5′ leader attenuator (◇); and strain MO205, a *pyr-lacZ* fusion including the *pyr* promoter, the 5′ leader attenuator, *pyrR*, the *pyrR*:*pyrP* attenuator and the 5′ half of *pyrP* (○). (C) β-Galactosidase accumulated by *pyr-lacZ* integrants analogous to those described for panel B except in a Δ*pyrR* background: DBR207, including the *pyr* promoter only (□); DBR290, including the *pyr* promoter and the 5′ leader attenuator (◇); and DBR205, including the *pyr* promoter plus the 5′ leader attenuator, *pyrR*, the *pyrR*:*pyrP* attenuator, and the 5′ half of *pyrP* (○).

this fusion integrant was compared with that of strain MO207, in which only nt −51 to +72 of *pyr* DNA (i.e., no Spo0A boxes [Table 6]) was fused to *lacZ* (Fig. 3A). The level of *pyr-lacZ* expression was about 30% higher in strain MO203 than in MO207 as seen on chemically defined medium (Table 6), but both strains showed the same pattern of β-galactosidase synthesis. In particular, both strains continued to accumulate β-galactosidase at equivalent rates during the stationary phase; no developmental shutoff of *pyr-lacZ* expression was observed (Fig. 3A). To test further any possible involvement of the *spo0A* gene in *pyr* regulation, strains MO203 and MO207 were transformed to obtain their *spo0A*::*cat* counterparts, as described in Materials and Methods. The corresponding strains, MO203A and MO207A, showed patterns of *pyr-lacZ* expression that were very similar to one another and to the fusions in a *spo0A*$^+$ background (Fig. 3A). These results argue strongly against participation of the Spo0A protein and the putative 5′ flanking Spo0A binding sites in regulation of *pyr* gene expression during early stationary phase. Subsequently, we became aware of the finding of Devine et al. (12) that regulation of expression of the *B. subtilis arg* operon by *spo0A* was observed in cells grown on solid medium but not in liquid medium. Accordingly, we repeated the experiments described in Fig. 3A, assaying β-galactosidase from cells grown on and harvested from rich medium agar plates, using procedures kindly communicated to us by K. M. Devine. Once more, no significant difference in accumulations of β-galactosidase in stationary cells of strains MO203, MO203A, MO207, and MO207A was observed (data not shown).

Next, we investigated whether the first and second attenuators of the *pyr* operon might play a role in developmental regulation. Strains MO1991 and MO205, which contain the *pyr* promoter and one or two attenuators, respectively, fused to *lacZ* (Table 4), were grown to stationary phase on rich medium, and β-galactosidase expression was compared with that of strain MO207, which contains the same promoter sequence but no attenuators (Fig. 3B). Both attenuator-containing *pyr-lacZ* fusion integrants showed a sharp reduction in the expression of β-galactosidase at the end of exponential growth. This shutoff in expression occurred earlier in the strain containing two attenuators, MO205. These results indicate that developmental regulation of *pyr* expression is actually related to repressive control of the operon, even though Maurizi and Switzer (32) demonstrated that intracellular pyrimidine nucleoside triphosphate pools decline in *B. subtilis* at the time of the shutoff of aspartate transcarbamylase synthesis.

If developmental control of *pyr* expression involves attenuators, it should also require a normal *pyrR* gene product. To

test this prediction, *pyr-lacZ* fusion plasmids containing the *pyr* promoter only; the *pyr* promoter and first attenuator; and the *pyr* promoter, first attenuator, an intact *pyrR* gene, and the second attenuator were integrated into the chromosome of a *B. subtilis* Δ*pyrR* strain. When these fusion integrants were grown on rich medium, developmental shutoff of *pyr-lacZ* expression did not occur in the promoter-only or promoter-plus-attenuator strains (Fig. 3C, DBR207 and DBR290) but was sharp and complete in the strain in which the fusion included a normal *pyrR* gene (DBR205). Thus, we conclude that the developmental regulation of *pyr* expression requires the participation of the PyrR protein acting on at least one and optimally two *pyr* attenuators. That is, developmental regulation must involve most of the same elements that operate during repressive control of *pyr* expression by exogenous pyrimidines during exponential growth.

DISCUSSION

A growing number of bacterial genes and operons are being found to be regulated by transcriptional attenuation mechanisms (4, 10, 11, 13, 14, 17, 18, 20, 23, 24, 28). The *B. subtilis pyr* operon is unique among those studied in that it contains three tandem attenuators. Prior to the present work, only the first (5′ leader) *pyr* attenuator had been shown experimentally to function in vivo (44). The second (*pyrR*:*pyrP*) and third (*pyrP*:*pyrB*) attenuators were identified by their sequences, which predicted their ability to fold as mRNA into mutually exclusive terminator and antiterminator stem-loop structures and from the lengths of transcripts on Northern blots, which were consistent with the mRNA species terminating at the predicted locations (44). The experiments reported here establish clearly that all three untranslated sequences of the *pyr* operon do contain pyrimidine-regulated transcriptional attenuators and that the regulation of each is completely dependent on the *pyrR*-encoded protein.

We sought to assess quantitatively the individual contributions of the three attenuators by isolating them and studying their regulation in *pyr-lacZ* fusion integrants. All were placed downstream from the normal *B. subtilis pyr* promoter. Even though the attenuators differ somewhat in nucleotide sequence and in the calculated stability of the stem-loops they are predicted to form (44), the extent of their regulation by exogenous uracil or during pyrimidine starvation was surprisingly constant. The third attenuator generally produced the highest levels of derepressed expression, but this was shown to be due to a small intercistronic open reading frame within the attenuator and not to the attenuator itself. Each attenuator was significantly repressed by the endogenous pyrimidines in cells growing on minimal medium. Only in pyrimidine-starved cells was the full range of expression revealed (34- to 57-fold for each attenuator in various experiments), but this range should be divided by a factor of about 2.5 to account for the attenuator-independent regulation observed under extreme pyrimidine limitation. That correction yields a regulatory range of 13- to 23-fold for each attenuator, which is still much larger than the 3- to 5-fold repression observed when comparing cells grown with and without exogenous uracil. There may well exist subtle differences in the sensitivities of the three attenuators to intracellular pyrimidine pools or variations in PyrR levels, but the present experiments do not reveal them.

The effect of combining the attenuators in tandem is twofold. First, it allows three regulatory step-down elements to be introduced into expression of the first genes of the operon. During pyrimidine starvation, all of the *pyr*-encoded proteins should be expressed at high levels. When pyrimidines are abundant, the series of attenuation steps ensures that some PyrR protein will be made, as is needed for regulation; a reduced amount of uracil permease is produced to allow continued uptake of exogenous uracil; and virtually none of the biosynthetic enzymes are synthesized. Second, the presence of tandem attenuators allows a very large range of expression of the biosynthetic enzymes. For example, the level of aspartate transcarbamylase activity is 300 times higher in a Δ*pyrR* mutant than in fully repressed *pyr*$^+$ cells (44). The theoretically available cumulative regulatory range for three attenuators, each of which is capable of a 15-fold range, would be $15 \cdot 15 \cdot 15 = 3{,}375$-fold. The observed range of expression is not so large, but it is doubtful that our methods could determine low levels of expression accurately. Altogether, the *pyr* operon contains a very versatile regulatory mechanism capable of a broader range of expression than typical single-attenuator systems and capable of differential expression of the first two genes of the operon.

Our experiments indicate that the structural elements of the *pyr* operon involved in regulation of its expression by pyrimidine metabolites are exclusively limited to the three attenuators and the *pyrR*-encoded regulatory protein. The *pyr* promoter and sequences upstream of it are not required for regulation and can be replaced by another unrelated *B. subtilis* promoter. We did observe that *pyr-lacZ* and *spac-lacZ* transcriptional fusion integrants were expressed at increased levels in cells subjected to extreme pyrimidine limitation. An *epr-lacZ* fusion integrant showed an opposite response. We speculate that these effects result from an altered rate of transcriptional initiation or the early steps of elongation in response to sharply altered pools of ribonucleoside triphosphates. Whatever the mechanism of these effects, they vary from promoter to promoter and their physiological significance is not known.

The rapid shutoff of *pyr* expression observed within 1 h after *B. subtilis* cells enter stationary phase as a result of glucose exhaustion in rich sporulation medium (32) appears to involve the same fundamental mechanisms as repression by exogenous pyrimidines, because the results of this work clearly showed that the shutoff requires both the *pyrR*-encoded protein and at least one and optimally two or three attenuators. The shutoff could result from changes in the intracellular pools of metabolites that interact with the PyrR protein and cause it to promote transcription termination. Since these metabolites have not been identified by experiment yet, we can only speculate as to their identity. It is known that the intracellular pools of pyrimidine nucleoside triphosphates decline in the stationary phase under these conditions (32), so UTP and CTP are unlikely regulators. In a previous paper, we speculated that the substrates of the uracil phosphoribosyltransferase activity of PyrR served as regulators of attenuation (44). Specifically, it was suggested that UMP serves as the primary repressing metabolite by binding to PyrR and promoting its ability to shift the attenuators from antiterminator to terminator structures. It was further suggested that 5-phosphoribosyl-1-pyrophosphate (PRPP) could antagonize UMP binding to PyrR and thus favor antitermination. This speculative model predicts that the shutoff in *pyr* transcription during early stationary phase is due to an increase in intracellular UMP pools, a decrease in intracellular PRPP pools, or both. A very sharp decrease in the PRPP pool has been shown to occur upon glucose exhaustion of *B. subtilis* cells grown on a different medium (5). An alternative mechanism for increased repression by the PyrR protein during sporulation could involve posttranslational modification, such as phosphorylation, as has been found in other attenuation systems (10, 11, 24). Further evaluation of these ideas will require full characterization of

the elements that regulate the function of the PyrR protein in attenuation, which is in progress in our laboratory.

ACKNOWLEDGMENTS

We thank Alan Grossman for plasmid pJL62, chromosomal DNA from *B. subtilis* AG503, and the procedure for β-galactosidase assay; Jerry Grandoni for plasmid pDH32 and *B. subtilis* MO199; Ping Hu for constructing *pyrB* deletion strain HC11; Kevin Devine for communicating to us his procedure for studying regulation of gene expression by *spo0A* of cells grown on solid medium; John Helmann for sending us plasmid pDG148; Reinhold Bruckner for plasmid pWPB183; and Charles Turnbough for critical comments on the manuscript of this communication.

This research was supported by National Institutes of Health grant GM47112.

REFERENCES

1. **Anagnostopoulos, C., P. J. Piggot, and J. A. Hoch.** 1993. The genetic map of *Bacillus subtilis*, p. 425–461. *In* A. L. Sonenshein, J. A. Hoch, and R. Losick (ed.), *Bacillus subtilis* and other gram-positive bacteria: biochemistry, physiology, and molecular genetics. American Society for Microbiology, Washington, D.C.
2. **Anagnostopoulos, C., and J. Spizizen.** 1961. Requirements for transformation in *Bacillus subtilis*. J. Bacteriol. **81:**741–746.
3. **Babitzke, P., and C. Yanofsky.** 1993. Reconstitution of *Bacillus subtilis trp* attenuation *in vitro* with TRAP, the *trp* RNA-binding attenuation protein. Proc. Natl. Acad. Sci. USA **90:**133–137.
4. **Beijer, L., R. P. Nilsson, C. Holmberg, and L. Rutberg.** 1993. The *glpP* and *glpF* genes of the glycerol regulon in *Bacillus subtilis*. J. Gen. Microbiol. **139:**349–359.
5. **Bernlohr, D. A., and R. L. Switzer.** 1983. Regulation of *Bacillus subtilis* glutamine phosphoribosylpyrophosphate amidotransferase inactivation in vivo. J. Bacteriol. **153:**937–949.
6. **Bond, R. W., A. S. Field, and R. L. Switzer.** 1983. Nutritional regulation of degradation of aspartate transcarbamylase and of bulk protein in exponentially growing *Bacillus subtilis* cells. J. Bacteriol. **153:**253–258.
7. **Bruckner, R., O. Shoseyov, and R. H. Doi.** 1990. Multiple active forms of a novel serine protease from *Bacillus subtilis*. Mol. Gen. Genet. **221:**486–490.
8. **Burbulys, D., K. A. Trach, and J. A. Hoch.** 1991. Initiation of sporulation in *B. subtilis* is controlled by a multicomponent phosphorelay. Cell **64:**545–552.
9. **Contente, S., and D. Dubunau.** 1979. Characterization of plasmid transformation in *Bacillus subtilis*: kinetic properties and the effect of DNA conformation. Mol. Gen. Genet. **167:**251–258.
10. **Crutz, A. M., M. Steinmetz, S. Aymerich, R. Richter, and D. LeCoq.** 1990. Induction of levansucrase in *Bacillus subtilis*: an antitermination mechanism negatively controlled by the phosphotransferase system. J. Bacteriol. **172:** 1043–1050.
11. **Debarbouille, M., M. Arnaud, A. Fouet, A. Klier, and G. Rapoport.** 1990. The *sacT* gene regulating the *sacPA* operon in *Bacillus subtilis* shares strong homology with transcriptional antiterminators. J. Bacteriol. **172:**3966–3973.
12. **Devine, K. M., K. G. Woodson, and M. O'Reilly.** 1993. Regulation of ribose transport and citrulline biosynthesis by Spo0A, abstr. L2. Abstracts of the Seventh International Conference on *Bacillus*.
13. **Ebbole, D. J., and H. Zalkin.** 1987. Cloning and characterization of a 12-gene cluster from *Bacillus subtilis* encoding nine enzymes for *de novo* purine nucleotide biosynthesis. J. Biol. Chem. **262:**8274–8287.
14. **Ebbole, D. J., and H. Zalkin.** 1988. Detection of *pur* operon-attenuated mRNA and accumulated degradation intermediates in *Bacillus subtilis*. J. Biol. Chem. **263:**10894–10902.
15. **Ghim, S.-Y., and J. Neuhard.** 1994. The pyrimidine biosynthesis operon of the thermophile *Bacillus caldolyticus* includes genes for uracil phosphoribosyltransferase and uracil permease. J. Bacteriol. **176:**3698–3707.
16. **Ghim, S.-Y., P. Nielsen, and J. Neuhard.** 1994. Molecular characterization of pyrimidine biosynthesis genes from the thermophile *Bacillus caldolyticus*. Microbiology **140:**479–491.
17. **Gollnick, P.** 1994. Regulation of the *Bacillus subtilis trp* operon by an RNA binding protein. Mol. Microbiol. **11:**991–997.
18. **Grandoni, J. A., S. B. Fulmer, V. Brizzio, S. A. Zahler, and J. M. Calvo.** 1993. Regions of the *Bacillus subtilis ilv-leu* operon involved in regulation by leucine. J. Bacteriol. **175:**7581–7593.
19. **Grossman, A. (Massachusetts Institute of Technology).** Personal communication.
20. **Grundy, F. J., and T. M. Henkin.** 1993. tRNA as a positive regulator of transcriptional antitermination in *B. subtilis*. Cell **74:**475–482.
21. **Hanson, R. S., J. Blicharska, and J. Szulmajster.** 1964. Relationship between the tricarboxylic acid cycle enzymes and sporulation of *B. subtilis*. Biochem. Biophys. Res. Commun. **17:**1–7.
22. **Helmann, J. (Cornell University).** Personal communication.
23. **Holmberg, C., and R. Rutberg.** 1991. Expression of the gene encoding glycerol-3-phosphate dehydrogenase (*glpD*) in *Bacillus subtilis* is controlled by antitermination. Mol. Microbiol. **5:**2891–2900.
24. **Houman, F., M. R. Diaz-Torres, and A. Wright.** 1990. Transcriptional antitermination in the *bgl* operon of *E. coli* is modulated by a specific RNA binding protein. Cell **62:**1153–1163.
25. **Hu, P., and R. L. Switzer (University of Illinois).** Unpublished data.
26. **Ikuta, N., M. B. N. Souza, F. F. Valencia, M. E. B. Castro, A. C. G. Schenberg, A. Pizzirani-Kleiner, and S. Astolfi-Filho.** 1990. The α-amylase gene as a marker for gene cloning: direct screening of recombinant clones. Biotechnology **8:**241–242.
27. **Kuroda, M. I., D. Henner, and C. Yanofsky.** 1988. *cis*-Acting sites in the transcripts of the *Bacillus subtilis trp* operon regulate expression of the operon. J. Bacteriol. **170:**3080–3088.
28. **Landick, K., and C. L. Turnbough, Jr.** 1992. Transcriptional attenuation, p. 407–446. *In* S. L. McKnight and K. R. Yamamoto (ed.), Transcriptional regulation. Cold Spring Harbor Laboratory Press, Cold Spring Harbor, N.Y.
29. **Lerner, C. G., B. T. Stephenson, and R. L. Switzer.** 1987. Structure of the *Bacillus subtilis* pyrimidine biosynthetic (*pyr*) gene cluster. J. Bacteriol. **169:** 2202–2206.
30. **Lerner, C. G., and R. L. Switzer.** 1986. Cloning and structure of the *B. subtilis* aspartate transcarbamylase gene (*pyrB*). J. Biol. Chem. **261:**11156–11165.
31. **Lu, Y., N. Y. Chen, and H. Paulus.** 1991. Identification of *aecA* mutations in *Bacillus subtilis* as nucleotide substitutions in the untranslated leader region of the aspartokinase II operon. J. Gen. Microbiol. **137:**1135–1143.
32. **Maurizi, M. R., and R. L. Switzer.** 1978. Aspartate transcarbamylase synthesis ceases prior to inactivation of the enzyme in *Bacillus subtilis*. J. Bacteriol. **135:**943–951.
33. **Miller, J. H.** 1972. Experiments in molecular genetics, p. 353–355. Cold Spring Harbor Laboratory, Cold Spring Harbor, N.Y.
34. **Otridge, J., and P. Gollnick.** 1993. MtrB from *Bacillus subtilis* binds specifically to *trp* leader RNA in a tryptophan-dependent manner. Proc. Natl. Acad. Sci. USA **90:**128–132.
35. **Quinn, C. L., B. T. Stephenson, and R. L. Switzer.** 1991. Functional organization and nucleotide sequence of the *Bacillus subtilis* pyrimidine biosynthetic operon. J. Biol. Chem. **266:**9113–9127.
36. **Roland, K. L., C. Liu, and C. L. Turnbough, Jr.** 1988. Role of the ribosome in suppressing transcriptional termination at the *pyrBI* attenuator of *Escherichia coli* K-12. Proc. Natl. Acad. Sci. USA **85:**7149–7153.
37. **Sambrook, J., E. F. Fritsch, and T. Maniatis.** 1989. Molecular cloning: a laboratory manual, 2nd ed., p. A1. Cold Spring Harbor Laboratory Press, Cold Spring Harbor, N.Y.
38. **Sanger, F., S. Nicklen, and A. R. Coulson.** 1977. DNA sequencing with chain-terminating inhibitors. Proc. Natl. Acad. Sci. USA **74:**5463–5467.
39. **Shimotsu, H., and D. Henner.** 1986. Construction of a single-copy integration vector and its use in analysis of regulation of the *trp* operon of *Bacillus subtilis*. Gene **43:**85–94.
40. **Shimotsu, H., M. I. Kuroda, C. Yanofsky, and D. J. Henner.** 1986. Novel form of transcriptional attenuation regulates expression of the *Bacillus subtilis* tryptophan operon. J. Bacteriol. **166:**461–471.
41. **Shindler, D. B., and L. M. Prescott.** 1979. Improvements on the Prescott-Jones method for the colorimetric analysis of ureido compounds. Anal. Biochem. **97:**421–422.
42. **Stansly, P. G., R. G. Shepherd, and H. J. White.** 1947. Polymyxin: new chemotherapeutic agent. Bull. Johns Hopkins Hosp. **81:**43–54.
43. **Stemmer, W. P. C.** 1991. A 20-minute ethidium bromide/high-salt extraction protocol for plasmid DNA. BioTechniques **10:**726.
44. **Turner, R. J., Y. Lu, and R. L. Switzer.** 1994. Regulation of the *Bacillus subtilis* pyrimidine biosynthetic (*pyr*) gene cluster by an autogenous transcriptional attenuation mechanism. J. Bacteriol. **176:**3708–3722.
45. **Wang, L. F.** 1986. Ph.D. thesis. University of California, Davis, Davis.
46. **Yanisch-Perron, C., J. Vieira, and J. Messing.** 1985. Improved M13 phage cloning vectors and host strains: nucleotide sequences of the M13mp18 and pUC19 vectors. Gene **33:**103–119.
47. **Yansura, D. G., and D. J. Henner.** 1984. Use of the *E. coli lac* repressor and operator to control gene expression in *Bacillus subtilis*. Proc. Natl. Acad. Sci. USA **81:**439–443.
48. **Zytkovicz, T., and H. O. Halvorson.** 1972. Some characteristics of dipicolinic acid-less mutant spores of *Bacillus cereus*, *Bacillus megaterium*, and *Bacillus subtilis*, p. 49–52. *In* H. O. Halvorson, R. Hanson, and L. L. Campbell (ed.), Spores V. American Society for Microbiology, Washington, D.C.